



Supporting Online Material for

Structure of Nup58/45 Suggests Flexible Nuclear Pore Diameter by Intermolecular Sliding

Ivo Melčák, André Hoelz,* Günter Blobel*

*To whom correspondence should be addressed. E-mail: hoelza@rockefeller.edu (A.H.), blobel@rockefeller.edu (G.B.)

Published 23 March 2007, *Science* **315**, 1729 (2007)
DOI: 10.1126/science.1135730

This PDF file includes

Materials and Methods
Figs. S1 to S9
Table S1
References

Other Supporting Online Material for this manuscript includes the following:
(available at www.sciencemag.org/cgi/content/full/315/5819/1729/DC1)

Movies S1 to S3

SUPPORTING ONLINE MATERIAL

MATERIALS AND METHODS

Plasmid Preparation

Various expression constructs of Nup58, Nup54, and Nup62 were generated from *R. norvegicus* cDNAs. For single protein expression, DNA fragments were amplified by PCR and subcloned into the pET28a expression vector (Novagen), resulting in a fusion protein that contained an N-terminal thrombin-cleavable His₆-tag. For the expression of various Nup62 complexes, a modular tri-cistronic expression vector was engineered based on the pET28a expression vector, containing sequentially the coding sequences of Nup58, Nup54, and Nup62, separated by ~60-bp linkers that each encode for an additional ribosomal binding site. Nup58 was expressed as an N-terminal His₆-tag fusion protein that contained a thrombin protease cleavage site directly after the N-terminal His₆-tag.

Protein Expression and Purification

All constructs were expressed in either *E. coli* BL21(DE3) or BL21 Codon-Plus(DE3)-RIL (Stratagene) at 30°C in the presence of 0.2 mM isopropyl-thio-β-D-galactoside (IPTG). The proteins were batch purified via the N-terminal His₆-tag of Nup58 using a nickel affinity resin (HIS-Select nickel affinity gel, Sigma) followed by thrombin cleavage. The proteins were further purified on HiTrap Q HP and HiLoad 26/60 Superdex 200 prep grade columns (GE Healthcare). The gel filtration column was equilibrated either in a buffer containing 10 mM Tris-HCl, pH 8.0, 150 mM NaCl, 0.5 mM EDTA, and 1 mM DTT or in the same buffer supplemented with 24 mM CHAPS. For oligomerization analysis, the proteins were run on Superdex 200 10/300 GL (Nup62 complex) or Superdex 75 10/300 GL (Nup58/45) columns, equilibrated in a buffer containing 10 mM Tris-HCl, pH 8.0, 150 mM NaCl, 0.5 mM EDTA, and 1 mM DTT unless indicated otherwise.

Crystallization of the Nup58/45 Core Domain

Tetragonal crystals of Nup58/45 were grown at 23°C in hanging drops containing 1.5 μl of the protein and 1.5 μl of a reservoir solution consisting of 100 mM BisTris-HCl, pH 6.1, 600 mM

CaCl₂, and 2.7% (w/v) Benzamidine-HCl using the Nup62 core complex (Nup58, residues 327-415; Nup54, residues 346-494; and Nup62, residues 322-525) at a protein concentration of 6.5 mg/ml. They grew to their maximum size of 100 μm x 100 μm x 50 μm within 10 days. The crystal quality was substantially improved by microseeding. For cryoprotection, the tetragonal crystals were stabilized in 100 mM BisTris HCl, pH 6.1, 600 mM CaCl₂, and 1.3% (w/v) Benzamidine-HCl and sequentially transferred into stabilizing solutions that contained increasing amounts of glycerol up to a final concentration of 23% (v/v). In the last transfer step, the cryoprotection solution was supplemented with 500 mM NaBr, which substantially increased the durability of the crystals in the x-ray beam. Crystals were flash frozen in liquid nitrogen. The heavy atom derivatized crystals were prepared by adding 0.2 μl of 30 mM OsO₄ directly into the crystallization drop and incubated for 10 min.

Orthorhombic crystals of Nup58/45 were grown at 23°C in hanging drops containing 1.5 μl of the protein and 1.5 μl of a reservoir solution consisting of 100 mM sodium acetate, pH 4.0, 400 mM CdCl₂, and 20% PEG 400 using the Nup62 core complex (see above) at a protein concentration of 17 mg/ml. Prior to crystallization, the buffer of the Nup62 core complex was exchanged on a gel filtration column to 10 mM Tris-HCl, pH 8.0, 150 mM NaCl, 0.5 mM EDTA, 1 mM DTT, and 24 mM CHAPS. Crystals grew to their maximum size in 7 days. The crystals were flash frozen in liquid nitrogen-cooled liquid propane.

Data Collection and Structure Determination

x-ray diffraction data of both Nup58/45 core domain crystal forms were collected at the Advanced Light Source (ALS), Lawrence Berkeley National Laboratory (LBNL), beamline 8.2.2 (Table S1). X-ray intensities were processed using the HKL2000 denzo/scalepack package (S1), and the CCP4 program package (S2) was used for subsequent calculations. Phasing from an Os SAD x-ray diffraction data set derived from the tetragonal crystals in SHARP (S3), followed by density modification in DM (S2) with solvent flattening and histogram matching, yielded an electron density map of excellent quality. A model lacking only the last four residues of all four protomers was built with the program O (S4). The model was refined using CNS (S5), and the stereochemical quality of the model was assessed with PROCHECK (S6). The structure of the orthorhombic crystals was solved by molecular replacement using the

coordinates of the dimer obtained from the tetragonal crystal form as a search model. The solution was independently validated with phases obtained from an Os SAD x-ray diffraction dataset, which were obtained similar to the phases of the tetragonal crystals (see above). The final model was refined to a 3.45 Å resolution with an R_{work} of 26.2% and an R_{free} of 31.0%, applying a 2σ structure factor cutoff ($F > 2\sigma F$). The final R values of the model are somewhat higher than would be expected based on the quality of the final model. Although the R_{work} increases sharply at about 3.6 Å, inclusion of all data to 3.45 Å resolution was beneficial in the interpretation of the electron density, and it was therefore decided not to truncate the data set to lower resolution. Data collection and refinement statistics are shown in Table S1.

Illustrations and figures

Figures were generated using PyMOL (S7). Molecular surfaces were calculated using MSMS (S8). Sequence alignments were generated using ClustalX (S9).

SUPPORTING REFERENCES

- S1. Z. Otwinowski, W. Minor, *Methods Enzymol.* **276**, 307-326 (1997).
- S2. Collaborative Computational Project, Number 4, *Acta Crystallogr. D Biol. Crystallogr.* **50**, 760 (1994).
- S3. E. de la Fortelle, G. Bricogne, *Methods Enzymol.* **276**, 472-494 (1997).
- S4. T. A. Jones, J. Y. Zou, S. W. Cowan, M. Kjeldgaard, *Acta Crystallogr. A* **47 (Pt 2)**, 110 (1991).
- S5. A. T. Brünger et. al., *Acta Crystallogr. D Biol. Crystallogr.* **54 (Pt 5)**, 905 (1998).
- S6. R. A. Laskowski, M. W. MacArthur, D. S. Moss, J. M. Thornton, *J. Appl. Crystallogr.* **26**, 283 (1993).
- S7. W. L. DeLano (2002); (www.pymol.org).
- S8. M. F. Sanner, A. J. Olson, J. C. Spehner, *Biopolymers* **38**, 305 (1996).
- S9. F. Jeanmougin, J. D. Thompson, M. Guoy, D. G. Higgins, T. J. Gibson, *Trends Biochem.* **23**, 403 (1998).

SUPPORTING TABLES

Table S1. Data collection and refinement statistics

Crystal data			
Crystal dataset / Space group	1 / $P4_322$ - Os a = b = 92.7 Å, c = 169.7 Å	2 / $P4_322$ - native a = b = 92.7 Å, c = 169.6 Å	3 / $C222_1$ - Os a = 132.9 Å, b = 230.2 Å, c = 131.8 Å
Unit cell parameters	$\alpha = \beta = \gamma = 90^\circ$	$\alpha = \beta = \gamma = 90^\circ$	$\alpha = \beta = \gamma = 90^\circ$
Asymmetric unit content	4 protomers	4 protomers	18 protomers
Solvent content (%)	70.7	70.7	52.3
Data collection statistics			
Beam line	ALS, BL 8.2.2	ALS, BL 8.2.2	ALS, BL 8.2.2
Wavelength (Å)	1.13973 (Os peak)	1.00813	1.13989 (Os peak)
Resolution range (Å)	50-3.25	20-2.85	20-3.45
R_{sym} (%)	11.1 (63.5)*	9.8 (38.9)*	6.9 (16.8)*
$\ \sigma(I) \ $	10.3 (2.0)*	12.7 (3.3)*	12.3 (5.4)*
Reflections measured / unique	590,605 / 12,454	475,371 / 18,077	777,174 / 26,835
Completeness (%)	96.4 (93.3)*	95.7 (98.1)*	95.7 (96.6)*
Phasing (crystal 1)			
Figure of merit (overall, SHARP)	0.334		
Figure of merit (after DM)	0.730		
Refinement statistics (crystal 2)			
$R_{\text{free}}/R_{\text{working}}$ (%)		28.8/25.0	
Reflections (work/test sets)		14,597/1,611 (9.0%)	
Number of non-H atoms		2,935	
Number of water molecules		79	
RMSD bonds (Å)		0.008	
RMSD angles (°)		1.109	
Model quality (Ramachandran Plot)			
Most favored (%)		95.7 (314)**	
Additionally allowed (%)		4.3 (14)**	
Generously allowed (%)		0.0 (0)**	
Disallowed (%)		0.0 (0)**	

* Parentheses refer to the highest resolution shell

** Parentheses refer to the number of residues

SUPPORTING FIGURES

Figure S1. Gel filtration profiles of Nup58/45³²⁷⁻³⁹⁹ at the indicated protein and salt concentrations. The elution positions for molecular weight standards are shown, and the predicted dimer and tetramer positions are indicated.

Figure S2. Analysis of the crystal content. SDS-PAGE gel illustrating the content of the tetragonal and orthorhombic crystals and the remaining solution of the crystallization drops. Both crystal forms only contain Nup58/45, while Nup62, Nup54, and excess Nup58/45 remain un-proteolyzed in the drop.

Figure S3. Molecular details of the dimerization interface. The C α traces of protomer A (green) and B (gray) are shown in coil representation, and the interface residues are shown in ball-and-stick representation. A pseudo-two-fold axis (red) runs vertically through the dimerization interface. For clarity, only residues of protomer A are labeled.

Figure S4. Structures of tetrameric Nup58/45 assemblies from the orthorhombic crystal form. **(A)** Ribbon representations of the two tetrameric Nup58/45 assemblies found in the orthorhombic crystal form. The asymmetric unit of the crystal contains 3 and 4 Nup58/45 tetramers of conformer 3 (dark red) and conformer 4 (teal), respectively. 90° rotated views are shown on the right. The location of the crystallographic two-fold axis (orange) in conformer 3, the non-crystallographic two-fold axis (blue) in conformer 4, and symmetry-related protomers are indicated. Conformer 3 and 4 are formed by protomers A and B, and their symmetry related protomers A' and B', and protomers C, D, E, and F, respectively. **(B)** Superposition of the two tetrameric Nup58/45 conformers. The unique protomers of the two tetrameric assemblies are superimposed onto protomer A of conformer 1 to highlight the lateral shift between the different conformers. For clarity, only one protomer of each superposition is colored. The N- and C-termini are labeled according to (A).

Figure S5. Surface conservation of vertebrate Nup58/45 homologs. **(A, B)** Surface representations of the oligomerization interfaces. The surface of the dimerization interface of one protomer (A) and the tetramerization interface of the dimer subunit (B) are shown. The conservation of the surfaces is indicated by a color gradient from white (60% identity) to dark green (100% identity). The associated α -helices are depicted as orange coil representations.

Figure S6. Sequence analysis of vertebrate Nup58/45. **(A)** Multiple sequence alignment of Nup58/45 from different species. The secondary structure elements are indicated as orange cylinders (α -helices), orange lines (coil regions), and solid orange circles (disordered residues). Numbering is relative to *Rattus norvegicus* Nup58. The sequence conservation is shown in a color gradient from light yellow (60% identity) to dark green (100% identity). The participation of various residues in the formation of the two interfaces is indicated by open circles (dimer interface) and solid triangles (tetramer interface). The conserved region of the tetramerization interface is boxed. The abbreviations for the sequences are: *Rattus norvegicus* (RATN), *Mus musculus* (MUSM), *Homo sapiens* (HOMS), *Pan troglodytes* (PANT), *Macaca fascicularis* (MACF), *Bos taurus* (BOST), *Canis familiaris* (CANF), *Gallus gallus* (GALG), *Xenopus laevis* (XENL), *Xenopus tropicalis* (XENT), *Danio rerio* (DANR), and *Tetraodon nigroviridis* (TETN). **(B)** Helical wheel representation illustrating the electrostatic character of the Nup58/45 N-helix (residues 332 to 355). The involvement of the residues in the formation of the various interfaces is labeled according to (A).

Figure S7. Sequence analysis of vertebrate Nup54. **(A)** Multiple sequence alignment of Nup54 from different species. Numbering is relative to *Rattus norvegicus* Nup54. The alignment is color-coded according to Figure S6. The abbreviations for the sequences are: *Rattus norvegicus* (RATN), *Homo sapiens* (HOMS), *Pan troglodytes* (PANT), *Macaca mulatta* (MACM), *Macaca fascicularis* (MACF), *Bos taurus* (BOST), *Mus musculus* (MUSM), *Gallus gallus* (GALG), *Xenopus laevis* (XENL), *Xenopus tropicalis* (XENT), and *Tetraodon nigroviridis* (TETN). The potential involvement of predicted helical residues in non-polar (black stars) and electrostatic interactions (red stars) is indicated. Residues arranged in the helical wheel representation (B) are boxed. **(B)** Helical wheel representation illustrating the electrostatic

character of two Nup54 α -helices that potentially form sliding regions similar to Nup58/45. The involvement of the residues in the formation of the non-polar and electrostatic interfaces is indicated and labeled according to (A).

Figure S8. Sequence analysis of vertebrate Nup62. **(A)** Multiple sequence alignment of Nup62 from different species. Numbering is relative to *Rattus norvegicus* Nup62. The alignment is color-coded and labeled according to Figure S6. The abbreviations for the sequences are: *Rattus norvegicus* (RATN), *Homo sapiens* (HOMS), *Pongo pygmaeus* (PONP), *Macaca fascicularis* (MACF), *Mus musculus* (MUSM), *Bos taurus* (BOST), *Canis familiaris* (CANF), *Gallus gallus* (GALG), *Xenopus laevis* (XENL), *Xenopus tropicalis* (XENT), *Danio rerio* (DANR), *Tetraodon nigroviridis* (TETN), and *Oncorhynchus mykiss* (ONCM). **(B)** Helical wheel representation illustrating the electrostatic character of two Nup62 α -helices potentially form sliding regions similar to Nup58/45. The involvement of the residues in the formation of the non-polar and electrostatic interfaces is indicated and labeled according to (A).

Figure S9. Sequence alignments of predicted sliding α -helices of Nup54 and Nup62 across eukaryotes. **(A)** Multi-species sequence alignment of helix A of Nup54 (see fig. S7) and **(B)** of helix A1 and A2 of Nup62 (see fig. S8). Numbering is relative to *Rattus norvegicus* Nup54 and Nup62. The alignment is color-coded using the BLOSUM 62 matrix from white (40% similarity) to red (100% similarity), and labeled according to figs. S7-8. Color bar represents metazoans (light blue), fungi (dark blue) and plants (green). The abbreviations for the sequences are: *Aedes aegypti* (AEDA), *Anopheles gambiae* (ANOG), *Apis mellifera* (APIM), *Arabidopsis thaliana* (ARAT), *Ashbya gossypii* (ASHG), *Aspergillus clavatus* (ASPC), *Aspergillus fumigatus* (ASPF), *Aspergillus nidulans* (ASPN), *Aspergillus oryzae* (ASPO), *Aspergillus terreus* (ASPT), *Bos taurus* (BOST), *Candida albicans* (CANA), *Candida glabrata* (CANG), *Canis familiaris* (CANF), *Chaetomium globosum* (CHAG), *Danio rerio* (DANR), *Debaryomyces hansenii* (DEBH), *Drosophila melanogaster* (DROM), *Drosophila pseudoobscura* (DROP), *Gallus gallus* (GALG), *Giberella zeae* (GIBZ), *Homo sapiens* (HOMS), *Hydra vulgaris* (HUDV), *Kluyveromyces lactis* (KLUL), *Macaca fascicularis* (MACF), *Macaca mulatta* (MACM), *Magnaporthe grisea* (MAGG), *Mus musculus* (MUSM), *Neosartorya fischeri* (NEOF),

Neurospora crassa (NEUC), *Oncorhynchus mykiss* (ONCM), *Pan troglodytes* (PANT), *Phaeosphaeria nodorum* (PHAN), *Pongo pygmaeus* (PONP), *Rattus norvegicus* (RATN), *Saccharomyces cerevisiae* (SACC), *Schizosaccharomyces pombe* (SCHP), *Strongylocentrotus purpuratus* (STRP), *Tetraodon nigroviridis* (TETN), *Tribolium castaneum* (TRIC), *Ustilago maydis* (USTM), *Xenopus laevis* (XENL), *Xenopus tropicalis* (XENT) and *Yarrowia lipolytica* (YARL).

ONLINE MOVIES

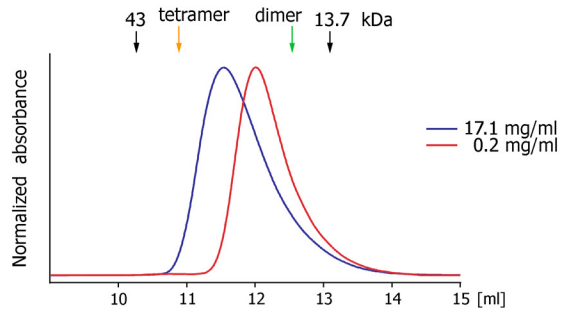
Movie S1. The sliding of dimeric subunits in Nup58/45 tetramers. The animation of four distinct states found in the tetragonal crystal form.

Movie S2. The sliding of dimeric subunits in Nup58/45 tetramers. The animation of four distinct states found in the orthorhombic crystal form.

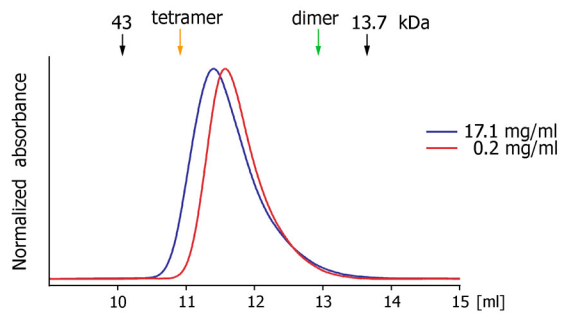
Movie S3. The detailed view of two sliding Nup58/45 N-helices. Each of the conformation states is described in Fig. 3 of the main text.

Figure S1

150 mM NaCl



50 mM NaCl



20 mM NaCl

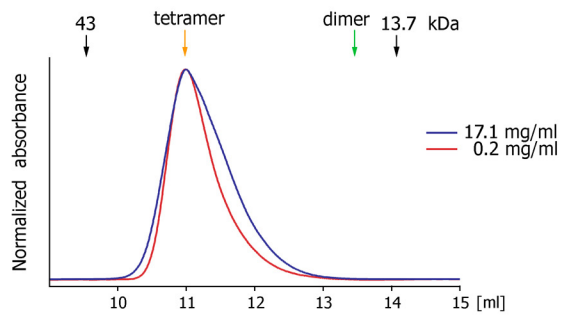


Figure S2

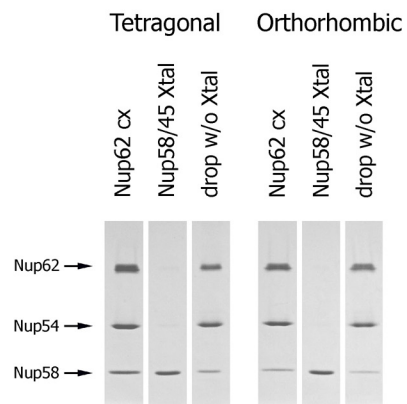


Figure S3

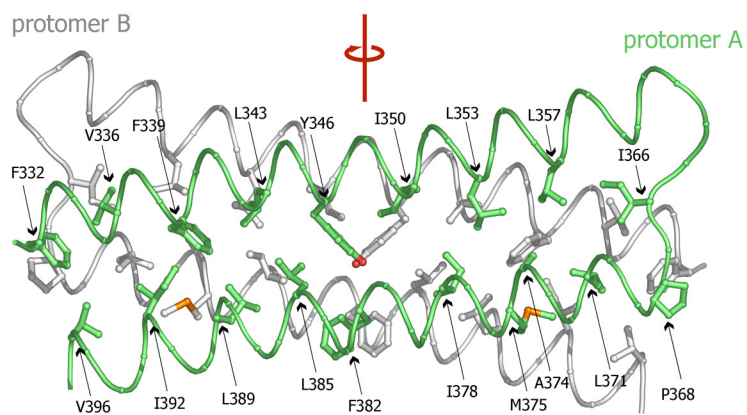


Figure S4

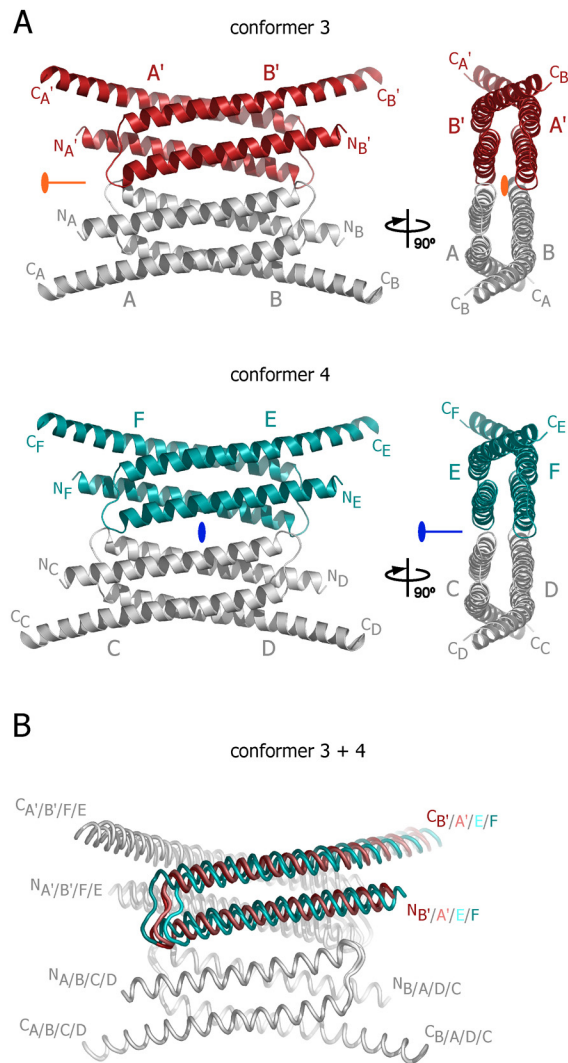


Figure S5

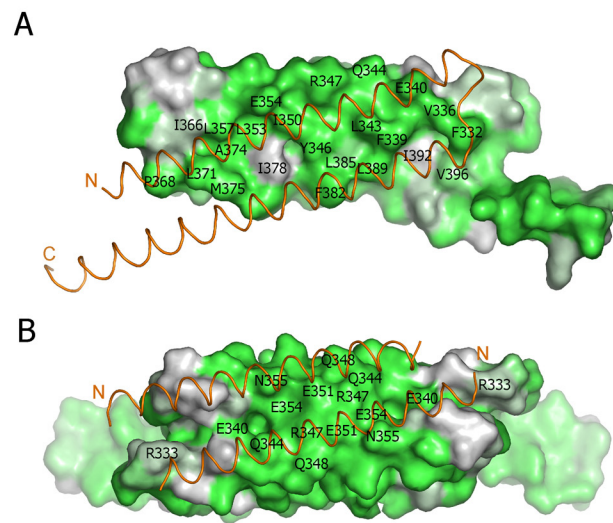
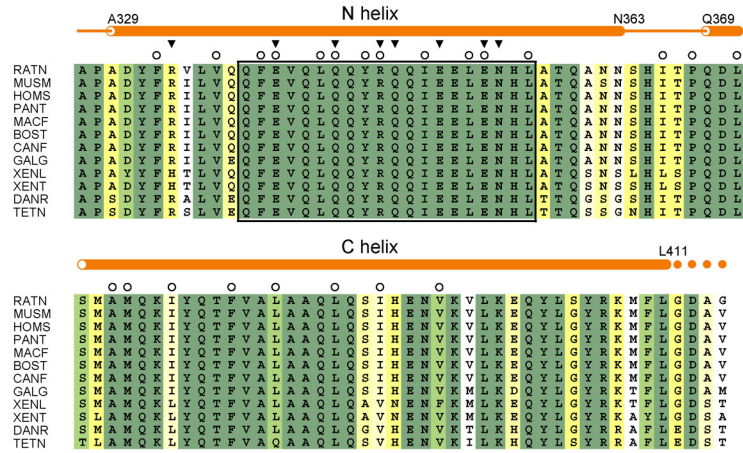


Figure S6

A Nup58/45



B Nup58/45 N helix (residues 332-357)

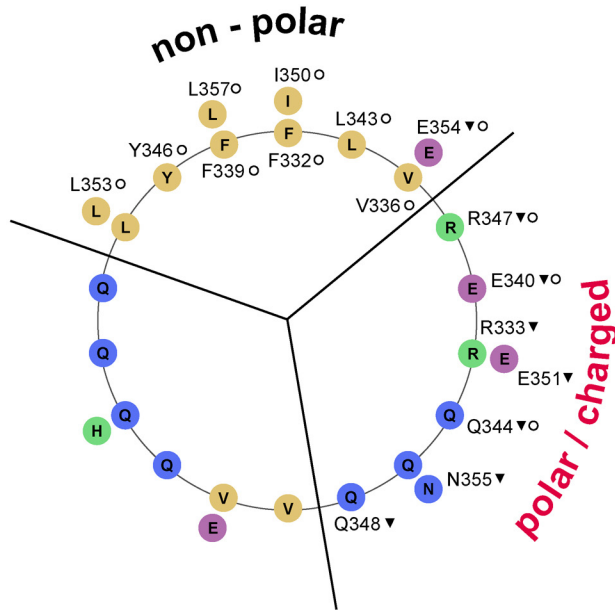
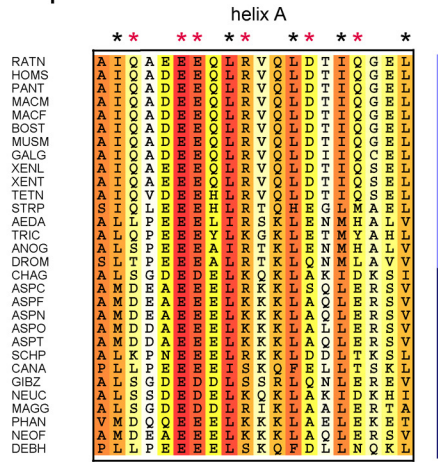


Figure S9

A Nup54



B Nup62

